Optimal design and operational tests of a high-temperature PEM fuel cell for a combined heat and power unit

Félix Barreras[1,*], Antonio Lozano[1], Vicente Roda[1,2], Jorge Barroso[1], Jesús Martín[1]

[1] *Laboratorio de Investigación en Fluidodinámica y Tecnologías de la Combustión, LIFTEC, CSIC-Universidad de Zaragoza, Maria de Luna 10, 50018 – Zaragoza (Spain)*

[2] *Instituto de Robótica e Informática Industrial, CSIC-UPC, Llorens i Artigas 4-6, 08028 – Barcelona (Spain)*

Abstract

Development of new materials for polymer electrolyte membranes has allowed increasing the operational temperature of PEM fuel cell stacks above 120°C. The present paper summarizes the main results obtained in a research devoted to the design, fabrication and operational tests performed on a high-temperature PEMFC prototype. A 5-cell stack has been assembled with commercial Celtec P-1000 high-temperature MEAs from BASF Fuel Cells, but the rest of elements and processes have been developed at LIFTEC research facilities. The main innovations of the present study are related to the design of the stack, and to the manufacturing and operation procedures. The novelties in the design include the flowfield geometry for both anode and cathode plates, the way in which reactant gases are supplied to the flowfield, the concept of block that eases the assembly and maintenance processes, and the heating strategy for a very fast start-up. The changes introduced to the assembly, closing and conditioning procedures are extensively described and discussed in the manuscript and contribute to the improvement in the stack performance. Results obtained in the preliminary operational tests performed are very promising, and it is expected that the 30-cells HT-PEMFC stack will deliver an electric power 2.3 times larger than the one initially predicted.

Keywords: Fuel Cells, PEM, High-temperature, Bipolar plates, Hydrogen

[*] Corresponding author: felix@litec.csic.es
Ph.: (+34) 976 506 520. Fax: (+34) 976 506 644

1.- INTRODUCTION

Nowadays, production of energy worldwide is mainly achieved by combustion of fossil fuels. Depletion of fossil fuel resources and pollution of the environment by the emission of solid particles and greenhouse gases have caused an increasing interest in the development of high efficiency energy generation devices [1-5]. This matter is particularly important in countries like Spain where lack of primary sources (mainly oil and natural gas), social rejection to nuclear power plants, and saturation of hydroelectric plants have led to a strong dependence on foreign Countries.

A well known highly efficient technology to generate electricity and thermal energy from a single fuel source is co-generation, also known as CHP (combined heat and power). This approach can also be used in a decentralized way, improving energy efficiency, security in energy supply, and reduction of CO_2 emissions. The EU and National Governments encourage the use of micro-combined heat and power systems (μ-CHP), in order to meet international and domestic targets on carbon emissions. For example, it is expected that by 2050 μ-CHP systems could provide 30–40% of the UK electricity needs [6]. To achieve this goal, the UK Government has lowered VAT from 17.5% to 5% for households that install μ-CHP systems, and has increased the planned reduction of carbon emissions for households up to 60% by 2050. In the same way, the Dutch Government is promoting similar initiatives and made public funding available to companies developing mass-market CHP systems [7]. μ-CHPs are especially interesting for small family houses (SFH) and medium family houses (MFH), small buildings and small and medium scale enterprises (SME) due to the very low noise and vibration levels. As both electricity and thermal energy demands fluctuate seasonally and hourly in residential buildings, it is necessary to take into account operational strategies for the variations in load demands. Then, it is necessary to develop a rational method of determining the size of the systems, as well as the operational strategies throughout the year [8].

As the minimum required temperature in buildings may vary between 40°C and 80°C, an output temperature close to 100°C is a convenient value for a μ-CHP system. In this context, fuel cells based on proton-exchange membranes (PEMFC) have many attractive features, such as their high power density, rapid start-up, and high efficiency, which make them a promising clean energy technology [9]. Recent progress in this type of PEMFCs has been focused on the development of devices that operate above 120°C, which are usually called high-temperature PEM fuel cells (HT-PEMFC). The operation of proton-exchange membrane fuel cells at high-temperature provides several advantages over traditional low-temperature ones. On the one hand, the

electrochemical kinetics for both anode and cathode reactions are enhanced enabling a potential reduction in the amount of noble metal catalyst used and an increase in the CO tolerance that allows the use of lower quality reformed hydrogen. At the same time, water management is simplified because only water in vapor phase has to be considered, preventing cells from flooding and simplifying the flowfield design. Finally, under these operating conditions, HT-PEMFCs are very simple and reliable devices because complicated humidification subsystems can be avoided, and cooling systems are drastically simplified due to the increase in temperature gradient between fuel cell stack and coolant.

This work is focused on the design, fabrication, and operational test of a HT-PEMFC stack that will be used as a CHP-device for residential applications. To this end, the heat extracted to the stack by the cooling system will be properly mixed with a cold air stream in order to fix the suitable comfort temperature into the house. The electric power is restricted to 1-3 kW that corresponds to the usual load for houses or small residential units. Although commercial MEAs are used, the stack includes several innovations, in particular the way in which reactant gases are supplied to the flowfield, the design of the flowfield geometry for both anode and cathode plates, the concept of blocks that eases the assembly and maintenance processes, and the heating strategy for a fast start-up.

2.- HT-PEMFC STACK DESIGN AND SYSTEMS

2.1 Monopolar plates. Flowfield geometry for reactant gases

It is evident that the dimensions of the flowfield geometry, and by extension those of the bipolar plates, are mainly influenced by the size of the membrane electrode assembly (MEA) to be used. For the present research, commercial Celtec®-P 1000 MEAs supplied by BASF Fuel Cells with a standard rectangular active area of 605 cm^2 have been selected. Celtec-P membrane consists of concentrated phosphoric acid associated in a polibenzimidazole (PBI) immobile gel phase. The operating temperature ranges from 120°C to 180°C, and no humidification for reactant gases is needed. The phosphoric acid is strongly associated to the PBI membrane matrix and this retains the acid in place, reducing the acid vapor pressure, and its evaporation. Platinum is used as catalyst in anode sides, and a special alloy is suited for the cathode electrodes. These MEAs have a very long-term stability, as well as a high CO tolerance, that makes them suitable for a vast range of practical applications. It should be noted that this type of MEA is highly hygroscopic. So, if the MEA is exposed to

humid air at room temperature, water is absorbed and the diluted phosphoric acid may tend to partially wash out and to migrate towards the plate channels. In the same way, contact to liquid water must be avoided, because it would slowly leach out the electrolyte [10].

Even when the operational characteristics of HT-PEMFCs allow the use of very simple bipolar plates (BP) flowfield geometries, a careful design of this element has been performed using the Navier-Stokes equations for mass and momentum conservation [11-13]. A "herringbone-type" geometry has been selected to cover the whole flowfield area [14]. A feature of this geometry, as depicted in Fig. 1, is that the total gas flow at the inlet port is divided, one half circulating downward to the lower-left corner, and the other half flowing along the channels oriented toward the upper-right corner of the active area. The advantage of this geometry with respect to another with a parallel serpentine is that the number of channels is increased, reducing the pressure drop and enlarging the electrical contact area between BP and gas diffusion layers (GDL). This leads to a drastic reduction of the pressure drop imposed by the channels to the flow of reactant gases, as well as a reduction in its average velocity. For example, considering two BPs with the same active area, one covered by a serpentine-parallel flowfield formed by 4 channels and the other by a "herringbone-type" one with also 4 channels of the same cross-sectional flow area and the same gas flow, the pressure drop imposed by the "herringbone-type" flowfield is 3.7 times less than that imposed by the serpentine-parallel one. At the same time, the average velocity of the reactant gas in the channels of the herringbone flowfield is almost twice less than that established at the serpentine-parallel channels.

To tackle the design of the flowfield geometry, the consumption of reactant gases has to be known. But together with the gas consumption based on the stack nominal electrical power, there are some other factors that must be considered. For example, the MEA manufacturer recommends that, in order to ensure the optimal lifetime of the device, for an electrical power in the range of 1-3 kW the number of cells in the stack should be between 30 and 35, and the voltage of each individual cell must be equal or larger than 0.4 V. So, considering a current density of 0.155 A cm^{-2}, which means a total current of 94 A, all the main parameters of the stack can be calculated. They are summarized in Table 1, where flow stoichiometry for hydrogen and oxygen are 1.2 and 2, respectively.

The optimal design of flowfield geometries includes the estimation of the pressure drop caused by the flowfield to the reactant gas flow. So, an initial channel diameter is assumed and both gas flow velocity and its Reynolds number are calculated. It is important to ensure that gas flow inside the channels is laminar, avoiding the formation

of turbulent structures that cause large energy dissipation. It should be noted that for the concept of monopolar plates used in this stack in both anode and cathode plates, flowfield geometries are manufactured only on one side. As it will be deeply explained below, anode plates are thinner with a flat surface in the back side, while cathode ones are thicker having the reactant gases distribution system and the channels for the cooling system in opposite sides. For the present monopolar plates (MPs), the "herringbone-type" flowfield that covers the active area (605 cm^2) is formed by 46 channels with a squared cross section of 1x1 mm^2, and a total length of 741 mm. A picture of the flowfield can be observed in Fig. 2. As in this case the active area is rectangular, channels cannot be aligned along the main diagonal, and have been slightly shifted.

Considering that the number of ribs is 45, and that they are 1 mm thick, 56.34% of the MEA active area (341 cm^2) is directly exposed to the reactant gases flow, while the remaining area (264 cm^2, representing 43.66% of the total) corresponds to the ribs ensuring the suitable electrical contact between plates and GDL. The total pressure drop that this "herringbone-type" flowfield imposes to the flow is 94.6 Pa for hydrogen in the anode sides, and 185.1 Pa for oxygen in the cathode ones.

Finally, in order to avoid some failures that are frequently observed, the MEA must be subjected to an appropriate compression rate. If it is over-compressed, a significant drop in OCV occurs due to electrical short circuits. On the other hand, if the MEA is under-compressed, the electrical contact between GDL and plate is insufficient. In order to avoid the positioning of hard-stops to prevent over-compression of the different MEAs as recommended by the manufacturer, a receding housing has been designed for these elements for an area of 250x300 mm^2 that includes the surrounding Kapton™ seal. So, the area where MEAs are housed has been lowered by 0.2 mm, in such a way that the maximum compression rate is 80% as recommended by the manufacturer, but simultaneously ensuring a good electrical contact.

Considering the application for this stack, a material with the highest possible thermal conductivity must be selected. Besides, having in mind that the excess of heat will be used for heating, different plates are used for anode and cathode sides, replacing the concept of bipolar plates by monopolar plates. In this case, MPs have been manufactured in aluminum Al-5083, which has low density (2700 kg cm^{-3}), and a good thermal conductivity (230 W m^{-1} K^{-1}). To avoid the well known problems when Al is exposed to the harsh environment of PEMFCs, the MP surface once manufactured has been coated with a very thin layer of chromium nitride (2.5 μm) by cathodic arc evaporation physical vapor deposition (CAE-PVD). This material is a ceramic coating,

but its thin micron-size thickness ensures the proper electrical conductivity required by these devices [15,16].

2.2. Reactant gases feeding system

Using a similar procedure to that described to design the flowfield geometry, the size of the main manifolds (inlet and outlet) for the circulation of the reactant gases has been calculated. To ensure a homogeneous gas distribution to every cell, the pressure drop to the gas flow caused by flowfield geometries must be 10 times larger than that imposed by manifolds [17,18]. With the calculated nominal flow of reactant gases, a rectangular cross section 10x130 mm^2 has been selected for the manifolds. So, for the nominal flow of hydrogen (34.4 Nl min^{-1}.) the pressure drop at the inlet manifold is 1.67 Pa, giving a ratio $\Delta P_{flowfield}/\Delta P_{manifold}$ of 56.5. For the oxygen nominal flow, 28.7 Nl min^{-1}, the pressure drop at the inlet collector is 0.49 Pa, resulting in a ratio $\Delta P_{flowfield}/\Delta P_{manifold}$ of 380.

Another innovation included in this stack is the way in which reactant gases are supplied to the flowfield geometry in both anode and cathode sides. Contrary to the typical design of gas feeding systems that can be consulted in the Literature, hydrogen and oxygen are supplied to the flowfield from the back-side of the MPs, as depicted in Fig. 3. To this end, a lowered step has been manufactured in the back-side of the cathode plates, which communicates the main gas manifolds with a thin slit that connects to the inlet section of the 46 channels that form the flowfield geometry. The access of reactant gases to reaction zones is simplified with this design, as well as the assembly of the different cells of the stack.

2.3. The sealing system

A good design of the sealing system of a PEMFC is always needed in order to avoid either gas leakage outside the device (very critical for hydrogen) or crossover between cathode and anode. Areas most favorable for leaking of reactant gases are the gas manifolds devoted to supply (or to exhaust) the reactants to (or from) the cells, and also the entire perimeter surrounding the flowfield geometry.

To avoid leakage of gases, in particular hydrogen, a rectangular channel 1.2 mm wide and 0.3 mm deep has been manufactured surrounding each gas manifold and the flowfield geometry, and a cord of a sealant material that supports the working temperature (above 150°C) has been deposited in it. The selected material, Loctite® 5910, is a single-component silicone-type adhesive that cures quite fast at room

temperature, becoming a flexible gasket which maintains its adhesive properties at different atmospheric conditions. Once cured, the joint has a Shore hardness of 30, with a volume resistivity of 1.69 x 10^{14} Ω-m, and surface resistivity of 2.81 x 10^{16} Ω-m. A good performance has been verified for this material in harsh environments with temperatures in the range from −50°C to +200°C, e.g. in car engine gaskets.

The silicone has been automatically deposited into the sealing channel using a 3-D Cartesian desktop I&J Fisnar I&J2500N dispensing robot. This equipment has a working area of 500x500 mm^2, and a continuous moving system with a positioning accuracy of 0.02 mm, and a maximum pressure of 150 bar. It can be easily programmed using a teaching pendant or an optional Windows® software. The final size of the gasket can be controlled by regulating the injection pressure, the exit diameter of the needle used, and the selected speed of displacement. A picture of this process is shown in Fig. 4.

2.4. The block system

Another novelty of this HT-PEMFC stack is its block system that solves most of the sealing problems observed in stacks composed by a large amount of cells. A benefit of this novelty is that the robustness of the final stack is improved easing the assembly process. At the same time, the maintenance time is shortened. For example, if some cells of the same block do not work properly (potential reduction or inversion) the entire block can be substituted by another one, or be removed from the stack in an easy way, and the stack can be back in service almost immediately.

A block of 5 cells is formed by 10 monopolar plates and 5 MEAs, and every individual cell is closed independently with 22 M4 screws. Since anode plates are thinner (only 2.5 mm thick), threads are machined on the cathode ones (5 mm thick). As every cell is closed independently, this strategy allows the use of a minimum closing force ensuring simultaneously the required compression of gaskets to avoid reactant gas leakage, as well as an excellent electrical contact between MP and GDL. Two pictures of a block are depicted in Fig. 5, where the different elements are represented in the left image, and the final appearance when it is already closed in the right one.

2.5. The preheating system

Another recommendation from the MEAs' manufacturer is that, in order to extend the lifetime of these elements and to ensure their suitable performance, the stack must

be heated up to 120°C before starting-up. It was therefore decided to place an electrical resistance wire in each of the plates to get the MEAs heated by conduction.

To make this process as efficient as possible, a channel has been machined in the front side of the anode MPs, as close as possible to the MEAs, as shown in Fig. 6. The selected electrical resistance is a single-polar heating wire coated with a double layer formed by an inner protection of silicone, externally shrouded by a metallic mesh plus a silicone cover. The 6 m long electrical resistance wires (one for each block) have an external diameter of 4 mm, and can dissipate a maximum power of 230 W. The size of the channel housing is 5.5 mm wide, in such a way that the outer diameter of the silicone protective coating of the electrical resistance can fit easily. When a cell is assembled, the electrical resistance wire is compressed between the two monopolar plates. As will be described in detail in the assembly section, the electrical resistance is long enough to be placed in the housing channel of the five anode MPs of the same block, continuously from one cell to another.

2.6. The excess of heat management system

As it has been previously discussed, the stack excess heat will be used to heat an isolated house. To ease the design, the excess heat management is performed by an air fan system, fixing the stack temperature around 160°C, as recommended for these MEAs. The optimal design of an air-cooling heat management system includes the correct dimensioning of the channels and a suitable selection of the air-fan system. The geometry of these channels is one of the most important factors to obtain a good performance of the fuel cell system. For simplicity and to ensure a low pressure drop [19,20], parallel straight channels are normally preferred in air-cooling systems.

To perform the optimal design of the heat management system it is necessary to calculate the amount of air needed to maintain the temperature of the stack in the working range as a function of the heat released. This has been performed using a 1D theoretical model formed by three submodels: one related to mass transfer phenomena, another one to characterize the electrochemical performance, and the thermal model itself [21]. Once the air flow is determined, the design of the geometry of the air cooling channels (length, height, and width) has to be accomplished, fixing also their number, using a set of Fluid Mechanic equations [20,21] to minimize the pressure drop by maximizing the air-cooling flow area. It has been verified that for the present application the air flow needed to maintain the stack temperature in the suitable working range when operating at the nominal electric power (a thermal load of 3.12 kW) is 2446.7 Nl min^{-1}. For this value, the calculated optimal channel system is that

formed by 24 channels, 5.5 mm wide, where the total pressure drop reaches the minimum value of only 64 Pa [21]. This channel configuration ensures 68% of electric contact area between two adjacent cells, which is also relevant to achieve a good performance of the electrochemical device. The rear side of a cathode MP with the air-cooling channels can be observed in the photo of Fig. 7.

When the optimal air-cooling channel configuration has been established based on the minimal pressure drop, suitable compact axial fans for the HT-PEMFC stack can be selected. As expected, the air-cooling flow rate required to remove the excess heat of the stack maintaining the adequate temperature, obtained from the 1D model, and the inherent pressure drop of the channels cannot be achieved with a single fan for moderate electric power consumption. For this stack, the selected cooling system is formed by three *ebm-papst* 612JH 12 V-DC fans [22] assembled in parallel configuration in suction mode, forcing the air to flow through the cooling channels. For the calculated pressure drop, the fan system can supply a maximum air flow of around 2900 Nl min^{-1} when rotating at the nominal speed (11700 r.p.m), with a low power consumption of 7.7 W for each fan. However, the flow rate propelled can be easily regulated by changing the supplied voltage in the range from 7 V to 12 V, in order to match the calculated air-cooling flow rate for the different thermal loads. The main parameters of the selected fans are summarized in Table 2.

3.- ASSEMBLY OF THE HT-PEMFC STACK

3.1. A greenhouse to control the relative humidity

As discussed in Section 2.1, the MEAs used in the present HT-PEMFC stack (Celtec P-1000) are very hygroscopic. For this reason, they are vacuum packed in factory inside a metallic vapor barrier bag. In order to achieve the very low humidity environment required by these MEAs during the assembly process, the zone dedicated to assemble the different cells has been isolated from the rest of the room by using a commercial greenhouse. A general picture of the outside of this facility, and two others from the inside are depicted in Fig. 8. To decrease the relative humidity inside the greenhouse, two pipes connected to the main air pressure line have been strategically placed just over the assembly table and the hydraulic press.

3.2. Assembly of a block of cells

In short, the assembly process of a block starts on the assembly table, placing PEEK washers in the machined groove around each screw of the anode plate that acts as the "endplate" of a block. This plate is different from the other anode MPs of the block because it is slightly larger, having holes at the four corners to allow the assembly with the adjacent block. Then, the MEA is placed in its housing and its entire perimeter is fixed to the plate with a Kapton™ tape. To prevent absorption of moisture, the face exposed to air is protected with a plastic sheet of its same size. Subsequently, the electrical resistance is placed in its housing, and is also fixed with Kapton. The remaining length of the exceeding wire of the electrical resistance will be subsequently placed in the housing of the other anode MPs of the block. An intermediate stage and the final form of an anode plate with all the elements assembled are shown in Fig. 9.

Once all the elements are assembled on the anode MP, it is moved to the hydraulic press, and placed on a special holder with four centering elements. The aim of this plate is to ensure the exact alignment of all the cells that form a block. With the anode plate exactly centered, a cathode MP is aligned over it, placing the side with the flowfield geometry over the MEA. Washers are now inserted in their housings, and M4 screws are used to assemble the two plates. Special PEEK® washers have been selected for the present application. This material retains its original shape for temperatures up to 180°C, and also offers a good resistance against most chemical environments.A small force (c.a. 5 bar) is then applied at the center of the plates with the hydraulic press to avoid its bending, and all screws are first tightened with a screwdriver, and when they are all fixed, a calibrated torque wrench is used to adjust the closing force to 1.5 N-m.

Once the assembly of the first cell of the block is finished, a new MEA protected with the piece of plastic is placed on its housing in the second anode plate in the assembly table and fixed to the plate with the Kapton tape. It is immediately moved to the hydraulic press and is perfectly aligned over the cathode plate. In this case, the back-side of the anode plate, with flat surface, faces the rear face of the cathode forming the cooling channels. Now, the excess wire of the electrical resistance is inserted in its housing and is also fixed to the plate with Kapton tape. After that, the second cathode MP is aligned over the anode one, and washers are inserted in their grooves. Once a small force is applied to the center of the plates, 22 new M4 screws are placed in the orifices being screwed, in the same way as before, to the cathode plate of the first cell, passing through the holes of the anode plate of the second cell.

Again, all screws are firstly tightened with the screwdriver, and the calibrated torque wrench is then used to adjust the torque to 1.5 N-m.

The assembling process for the second cell is exactly repeated for cells 3, 4 and 5. It should be noted that, once the 5 cells of the block are assembled, part of the wire of the electrical resistance must exceed, so that it can be electrically connected to the one in the next block. An example of a block during the assembly is depicted in Fig. 10, where the detail of the electrical resistance linking from one cell to another is zoomed in the insert at the upper right corner.

3.3. Closing procedure

The closing procedure for a single cell, a block, or the stack is basically the same. First of all, the electrical collector plates and the pressure-transmitter plates have to be electrically isolated using a flat silicone gasket 2 mm thick. The two pairs of electrical collector plates and the pressure-transmitter plates (with the silicone gasket in between) are independently screwed, in order to ease the final assembling process. Electrical collector plates must have an excellent electrical contact with both the anode plate of the first cell and the cathode plate of the last cell, respectively. Pressure-transmitter plates are 1 cm thick, and have threaded-orifices for all gas connectors, and those for the relative humidity sensors. Endplates have 20 passing-holes for M10 screws located on its periphery, as well as 13 threaded-holes also for M10 screws distributed in the central area.

Again, the hydraulic press is used to close the device. One of the endplates is positioned over the base of the hydraulic press, and one set of the electrical collector and pressure-transmitter plates is placed over it. Then, the block, the first if the stack is being assembled, is placed with the flat side of the first anode plate facing the electrical collector plate. Once the alignment is verified, the second set of electrical collector and pressure-transmitter plates is placed over the last cathode plate of the block. Subsequently, the other endplate is placed, and the 20 M10 screws are located in their orifices. Once all nuts are screwed by hand, a force of 20 bar is applied with the hydraulic press, and the tighten process starts following a "cross-scheme" applying a final closing torque of 20 N-m with the calibrated torque wrench.

Finally, the closing force for the 13 M10 screws placed on the zone corresponding to the active area is optimized using electrochemical impedance spectroscopy. For this purpose, an Autolab/PGSTAT302 with a frequency analyzer module FRA2 has been used, applying a current of 1 A and a voltage of 10 V through the collector plates of the block. The behavior of the internal Ohmic resistance, calculated when the imaginary

part of the impedance is 0, can be observed in Fig. 11. As can be seen, the overall Ohmic resistance of the block decreases from 27.22 mΩ to 12.73 mΩ when the closing force increases from 0 to 15 N-m. With this measurement, the importance of the central screws is clearly demonstrated, especially when MEAs with a large active area are used to form a stack.

There are several reasons that can explain possible discrepancies observed between the present resistance results and those typically reported in measurements performed in laboratory using single cells with very small active area [10,18]. First, the present measurements have been performed in a stack formed by 5 cells. Second, the inclusion of the cooling channels in monopolar plates reduces the electric contact area. Finally, the use of MEAs with very large active area (605 cm^{-2}) is another point to be considered because flatness of the whole area is very difficult to achieve, also affecting the total electric contact area. In any case, the improvement derived from the presence of the central screws in the end-plates has been demonstrated, but it is possible that the number of screws and their distribution over the main plane of the end-plates could be further optimized in future designs to ensure the transmission of a uniform force throughout the whole active area.

4.- EXPERIMENTS AND RESULTS

4.1. Conditioning of a 5-cell block

The first step before starting the conditioning procedure is to verify that there are no leaks of reactant gases neither out of the device nor between cathodes and anodes. This step has to be performed with dry gases (air or N_2) in order to avoid washing out of the electrolyte due to excessive contact with liquid water. Once checked, it is important to be sure that there are no traces of water or unwanted gases from previous tests in the gas lines. This is performed by purging both the anode and the cathode lines with a nitrogen flow of 0.05 Nl min^{-1} for 5 minutes. Then, the following procedure is followed:

1. The device (a single cell, a block, or the whole stack) must be heated up to 120°C for 2 hours using an external heat source.
2. A flow of 1 Nl min^{-1} of H_2 and O_2 is fed to the anode and cathode lines, respectively, in order to remove the remaining N_2, and to fill the channel of the flow geometry with reactant gases.
3. Finally, an initial flow for both reactant gases of 0.5 Nl min^{-1} has to be supplied.

4. Once the device is ready, the actual activation protocol must be performed following these steps:
    - Initially, a low voltage is fixed to the electronic load, so that the current generated by the device increases gradually.
    - Once the produced current exceeds 160 A, the electronic load working mode is changed to demand a constant current of 150 A, which corresponds to a current density of 0.25 A cm^{-2} for this MEA.
    - The demanded current is kept fixed in 150 A, and a gradual increase in the voltage of the device is programmed, until the value of 0.4 V/cell is exceeded.
    - When the voltage becomes constant, the device must be kept at this point for at least 10 hours, verifying that the electrical performance remains in steady state.
5. After these steps, the fuel cell is ready to be subjected to different charge demands, in order to complete a polarization curve.

4.2. Polarization curve of the 5-cell small stack

The polarization curve obtained for a small stack formed by 5-cells at a constant temperature of 160°C is shown in Fig. 12, together with two photos of the device when connected to the test bench during the test. To obtain the polarization (V *vs.* I) curve, the following points should also be considered. On the one hand, as the device should never be operated at open circuit voltage, a small current (0.05 A) must be drawn at the initial stage, in order to avoid the fast degradation of the cathode electrodes when exposed to high temperature and high potential conditions. After a given time, when it is considered that the device has reached steady state conditions, the demanded current can be increased step by step. The automatic gas supply unit of the test bench is regulated by software, ensuring that the stoichiometry of both hydrogen and oxygen flows is adjusted to 1.45 and 9, respectively for any value of current demanded by the electronic load.

First of all, some typical features can be observed in the polarization curve shown in Fig 12b. One striking point is that the zone corresponding to mass transfer losses common in low-temperature PEMFCs cannot be found, even after reaching current densities above 0.6 A cm^{-2}. This behavior can be explained due to the fact that in HT-PEMFCs water remains in vapor phase, easing its management, and reducing the blockage of the small GDL pores in the cathode sides. Besides, the 5-cell stack has been capable of supplying a maximum power close to 650 W, for a current of 330 A (0.545 A cm^{-2}), and a voltage of 0.4 V per cell, which is in the range recommended by

the manufacturer. Even when the maximum current density obtained is reasonably high for a stack formed by commercial MEAs with a large active area, higher values could be expected if the whole Ohmic resistance is reduced as commented in Section 3. However, if the current density is limited to 0.2 A cm^{-2} (121 A) in order to enlarge the lifetime of the device, the nominal power yielded by the 5-cells stack is 380 W, with a voltage of 0.6 V per cell.

There are some other points about the performance of the small stack with respect to the demanded current that should be commented. At the low current range, neither the heat produced by the stack nor the extra heat supplied by the electrical resistance wire are high enough to ensure the actual working temperature. It is for this reason that when the stack works at these points an external heating source (in the present experiments, a commercial air heater) must be kept working. On the contrary, once the demanded current exceeds 100 A (0.165 A cm^{-2}) the heat produced by electrochemical reactions is large enough to keep the stack temperature steady at 160°C, and both the external heat source and the electrical wire resistance can be disconnected. Finally, in the high current range (above 270 A, 0.45 A cm^{-2}), the heat yielded causes an increase in the stack temperature, reaching values as high as 200°C. It is in this last operational point where the three axial fans that constitute the air cooling system have to be switched on to cool down the stack. After that, the rotation speed of the axial fans has to be regulated in order to maintain the stack temperature around the nominal working value (160°C).

The experimental results obtained in the 5-cells small stack indicate that the 30-cells HT-PEMFC stack will be capable of delivering a nominal power around 2300 W, 65% better than the power estimated during the design procedure. This result could be obtained even restricting the current density to a maximum of 0.2 A cm^{-2}, which ensures a long lifetime of the device.

5.- CONCLUSIONS

In the present paper, the design, fabrication and operational tests performed on a high-temperature PEMFC for a CHP-unit have been described. Different innovations have been included as the “herringbone-type” flowfield geometry used in monopolar plates; the way in which reactant gases are supplied to the flowfield; the design of the flowfield geometry for both anode and cathode plates; the heating strategy that shortens the start-up time; and the concept of block that ease the assembly process.

Specific procedures have been established to optimize the assembly, closing and conditioning/activation stages of the stack. All of them are particularly relevant to ensure the optimal performance of the stack, especially because the commercial MEAs used in the stack are highly hygroscopic, and special care has to be considered to avoid a drastic reduction of the proton conductivity. The presence of screws at the end-plates in the central zone of the active areas of the MEAs has represented a relevant improvement that helps to homogenize the closing force, reducing the overall internal resistance of a 5-cell stack more than a 60% when the torque applied is increased from 0 to 15 N-m.

A maximum power of 650 W has been yielded by the small 5-cell stack. It is obtained for a current of 330 A, which corresponds to a current density of 0.545 A cm^{-2}. These preliminary results obtained indicate that the 30-cell HT-PEMFC stack could deliver a nominal total power around 2300 W, 2.3 times larger than that assumed during the design stage, confirming the relevance of the decisions taken during the design and assembly stages of this HT-PEMFC stack. This result could be obtained even restricting the current density to a maximum of 0.2 A cm^{-2}, which should extend the lifetime of the device. However, it is also expected that the actual power of the stack could be a bit lower than the one estimated, due to the increase in Ohmic losses introduced by the elements of the additional cells to be integrated. The total Ohmic resistance could be reduced optimizing the number and distribution of the central screws located in the end-plates. In this case, a higher maximum current density could be expected. Finally, lifetime tests will start in short, but in this case limiting the current density to 0.2 A cm^{-2} as suggested by the MEAs' manufacturer. With this, the effectiveness of the innovations considered during the design, and the relevance of the changes introduced to the different procedures will be assessed in more detail.

REFERENCES

1 U.S. Energy Information Administration, Annual Energy Review 2009; August 2010, DOE/EIS-0384

2 Crockett RGM, Newborough M, Highgate DJ. Electrolyser based energy management: a means for optimising the exploitation of variable renewable-energy resources in stand-alone applications. Solar Energy 1997; 61: 293–302

3 Wood G, Newborough M. Dynamic energy-consumption indicators for domestic appliances: environment, behavior and design. Energy Building 2003; 35: 821–841

4 Peacock AD, Newborough M. Impact of micro-combined heat and-power systems on energy flows in the UK electricity supply industry. *Energy* 2006; 31: 1468–1482

5 Santangelo PE, Tartarini P. Fuel cell systems and traditional technologies. Part I: Experimental CHP approach. Applied Thermal Engineering 2007; 27: 1278–1284

6 Cambridge Consultants Ltd, Cambridge Consultants UK, and Cambridge Consultants USA, available in: http://www.cambridgeconsultants.com/news_pr184.shtml

7 Kuhn V, Klemes J, Bulatov I. MicroCHP: Overview of selected technologies, products and field test results. Applied Thermal Engineering 2008; 28: 2039–2048

8 Ren H, Gao W, Ruan Y. Optimal sizing for residential CHP system, Applied Thermal Engineering 2008; 28: 514–523

9 Zhang J, Xie H, Zhang J, Tang Y, Song Ch, Navessin T, et al. High temperature PEM fuel cells. J. Power Sources 2006; 160: 872-891

10 Henskel C. Celtec®-P 1000 Membrane Electrode Assembly. Technical Information Brochure, D-BASF The Chemical Company, Frankfurt, August 2011

11 White F.M. Fluid Mechanics, 7th ed. New York: McGraw-Hill; 2011

12 Barreras F, Lozano A, Valiño L, Mustata R, Marín C. Fluid dynamics performance of different bipolar plates. Part I: velocity and pressure fields. J. Power Sources 2008; 175: 841-850

13 Lozano A, Valiño L, Barreras F, Mustata R. Fluid dynamics performance of different bipolar plates. Part II: flow through the diffusion layer. J. Power Sources 2008; 179: 711-722

14 Lincheta E, Barreras F, Lozano A, Valiño L, Mustata R. Bipolar plate with a flow-field topology “herringbone” type, Application Nº: P201031092, Priority Date: 16 July 2010

15 Barranco J., Barreras F, Lozano A, Lopez AM, V. Roda, Martin J, et al. Cr and Zr/Cr Nitride CAE-PVD Coated Aluminum Bipolar Plates for Polymer Electrolyte Membrane Fuel Cells. Intl. J. Hydrogen Energy 2010; 35: 11489–11498

16 Barranco J, Barreras F, Lozano A, Maza M. Influence of CrN-coating Thickness on the Corrosion Resistance Behaviour of Aluminium-based Bipolar Plates. J. Power Sources 2011; 196: 4283–4289

17 Mustata R, Valiño L, Barreras F, Gil MI, Lozano A. Study of the distribution of air flow in a proton exchange membrane fuel cell stack. J. Power Sources 2009; 192: 185-189

18 Barbir F. *Fuel Cells. Theory and Practice*, 1st ed. Burlington: Elsevier Academic Press; 2005

19 Barreras F, Lopez AM, Lozano A, Barranco J. Experimental Study of the Pressure Drop in the Cathode Side of Air-forced Open-cathode Proton Exchange Membrane Fuel Cell. Intl. J. Hydrogen Energy 2011; 36: 7612-7620

20 Lopez AM, Barroso J, Roda V, Barranco J, Lozano A, Barreras F. Design and development of the cooling system of a 2 kW nominal power open-cathode PEM fuel cell. Intl. J. Hydrogen Energy 2012; 37: 7289-7298

21 Barreras F, Lozano A, Barroso J, Roda V, Maza M, Theoretical model for the optimal design of air cooling systems of polymer electrolyte fuel cells. Application to a high-temperature PEMFC. Fuel Cells 2013; 13: 227-237

22 *ebmpapst* compact axial fan catalogue, available in: http://www.ebmpapst.com

TABLE CAPTIONS

Table 1. Summary of the main design parameters of the HT-PEMFC stack

Table 2. Main parameters of the fan selected for the cooling system of the stack

FIGURE CAPTIONS

Figure 1. Circulation of the reactant gases in the “herringbone-type” flowfield geometry

Figure 2. Herringbone-type flowfield geometry for both anode and cathode plates

Figure 3. Supply of reactant gases to the flowfield geometry

Figure 4. Gasket of the silicone Loctite® 5910 deposited in the housing around a gas manifold

Figure 5. Two pictures of a block showing the different elements (left), and its final form when it is already closed (right)

Figure 6. Positioning of the electric resistance wire around each MEA

Figure 7. Rear side of cathode MPs showing the six blocks of channels to control the stack temperature

Figure 8. Isolated greenhouse (right) to control the relative humidity during the assembly of blocks, and the location of the two pipes inside it (right)

Figure 9. Two images of the assembling process of a MEA in the first anode MP: intermediate stage protected with the plastic sheet (right), and its final form (left)

Figure 10. Assembly of a block at the hydraulic press, and a detail showing how the electrical resistance is mounted from one cell to another in the insert at the upper right corner

Figure 11. Internal Ohmic resistance as a function of the closing force of the central screws calculated using electrochemical impedance spectroscopy

Figure 12. Two images of the small stack of 5-cells in the test bench ready to be tested (a), and a polarization curve for a working temperature of 160°C (b)

TABLE CAPTIONS

Table 1. Summary of the main design parameters of the HT-PEMFC stack

Table 2. Main parameters of the fan selected for the cooling system of the stack

FIGURE CAPTIONS

Figure 1. Circulation of the reactant gases in the “herringbone-type” flowfield geometry

Figure 2. Herringbone-type flowfield geometry for both anode and cathode plates

Figure 3. Supply of reactant gases to the flowfield geometry

Figure 4. Gasket of the silicone Loctite® 5910 deposited in the housing around a gas manifold

Figure 5. Two pictures of a block showing the different elements (left), and its final form when it is already closed (right)

Figure 6. Positioning of the electric resistance wire around each MEA

Figure 7. Rear side of cathode MPs showing the six blocks of channels to control the stack temperature

Figure 8. Isolated greenhouse (right) to control the relative humidity during the assembly of blocks, and the location of the two pipes inside it (right)

Figure 9. Two images of the assembling process of a MEA in the first anode MP: intermediate stage protected with the plastic sheet (right), and its final form (left)

Figure 10. Assembly of a block at the hydraulic press, and a detail showing how the electrical resistance is mounted from one cell to another in the insert at the upper right corner

Figure 11. Internal Ohmic resistance as a function of the closing force of the central screws calculated using electrochemical impedance spectroscopy

Figure 12. Two images of the small stack of 5-cells in the test bench ready to be tested (a), and a polarization curve for a working temperature of 160°C (b)

Table

Parameter	Value	Unit
Electric power:	1.500	W
Number of cells:	30	-
Active area:	605	cm^2
Total voltage:	16	V
Total current:	94	A
Total H_2 consumption:	34.4	Nl min^{-1}
Total O_2 consumption:	28.66	Nl min^{-1}

Table 1. Summary of the main design parameters of the HT-PEMFC stack

Parameters	Value	Units
Nominal voltage	12	V
Speed rate	11700	min^{-1}
Input power	7.7	W
Maximum airflow rate	70	Nm^3/h
Noise level	53	dB(A)
Dimensions	60x60x32	mm^3

Table 2. Main parameters of the fan selected for the cooling system of the stack

Fig-1

Click here to download high resolution image

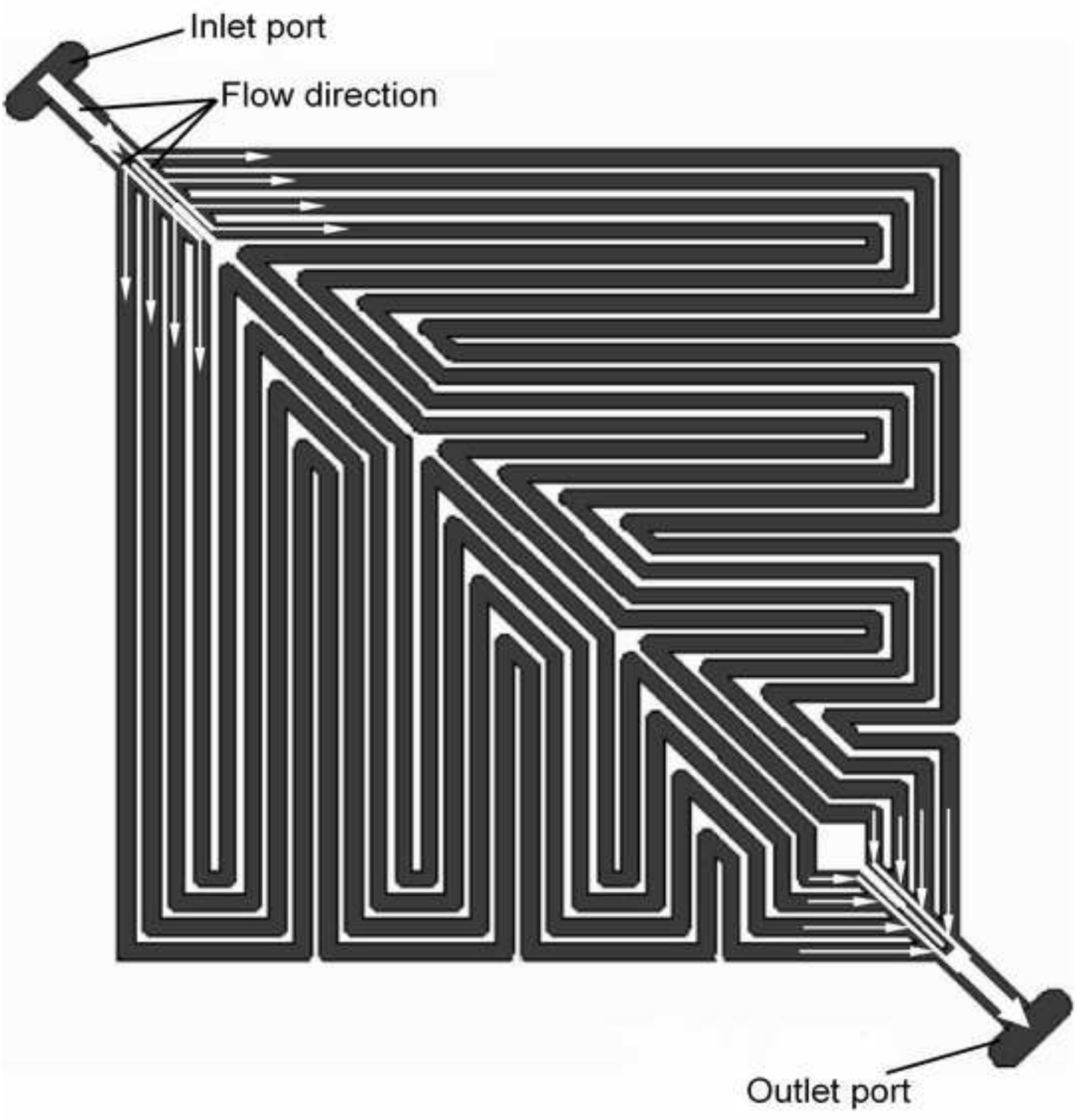

Fig-2

Click here to download high resolution image

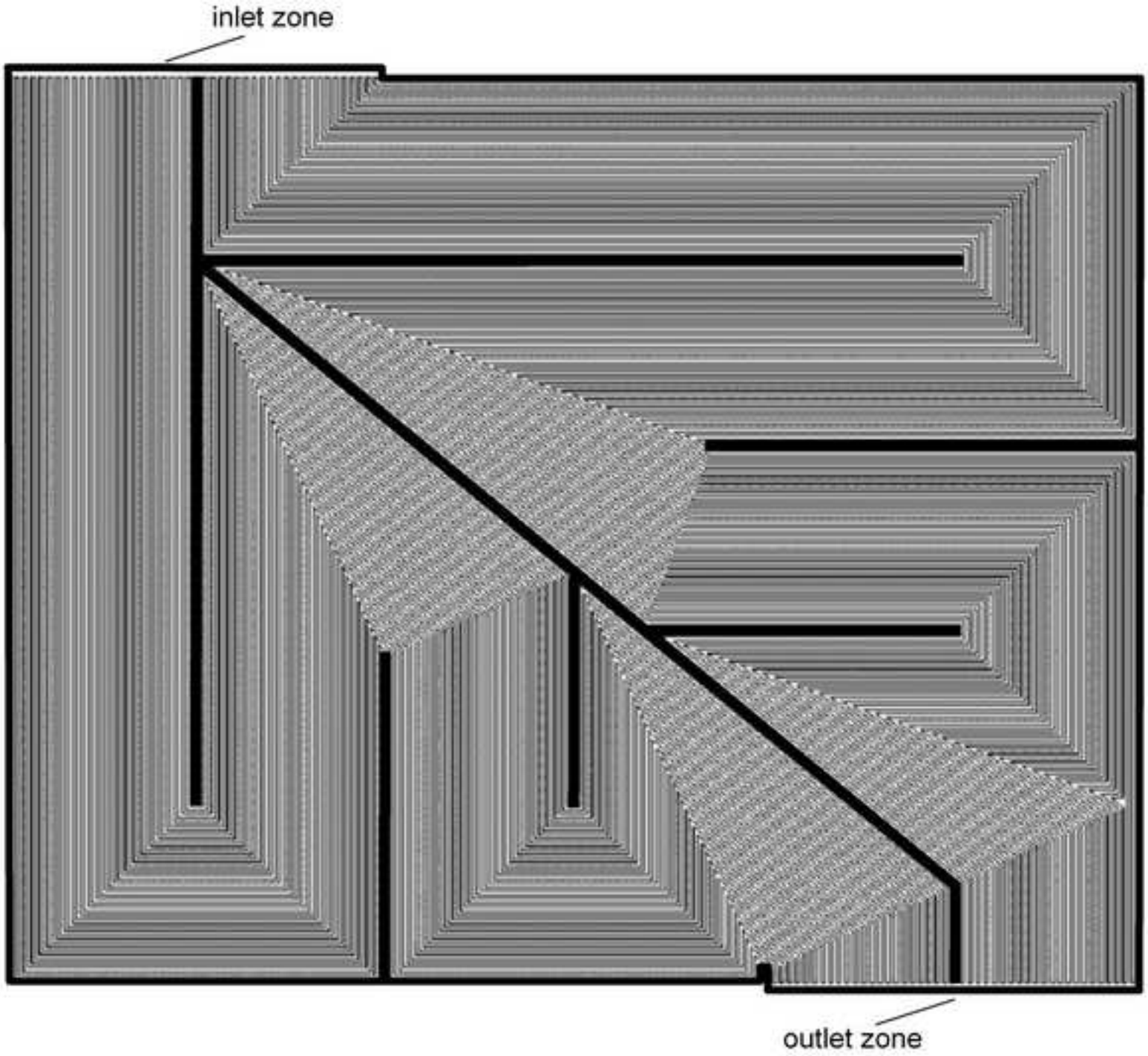

Fig-3

Click here to download high resolution image

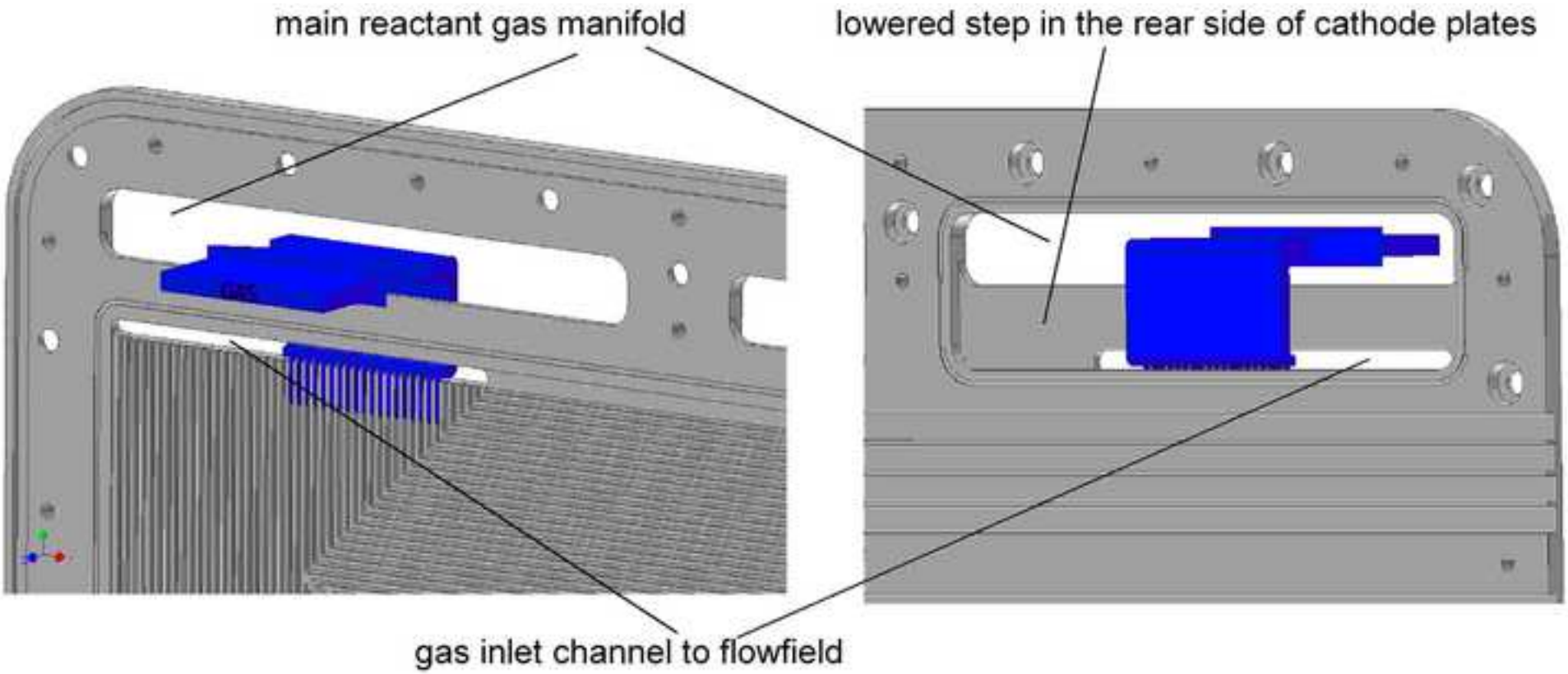

Fig-4

Click here to download high resolution image

Fig-5

Click here to download high resolution image

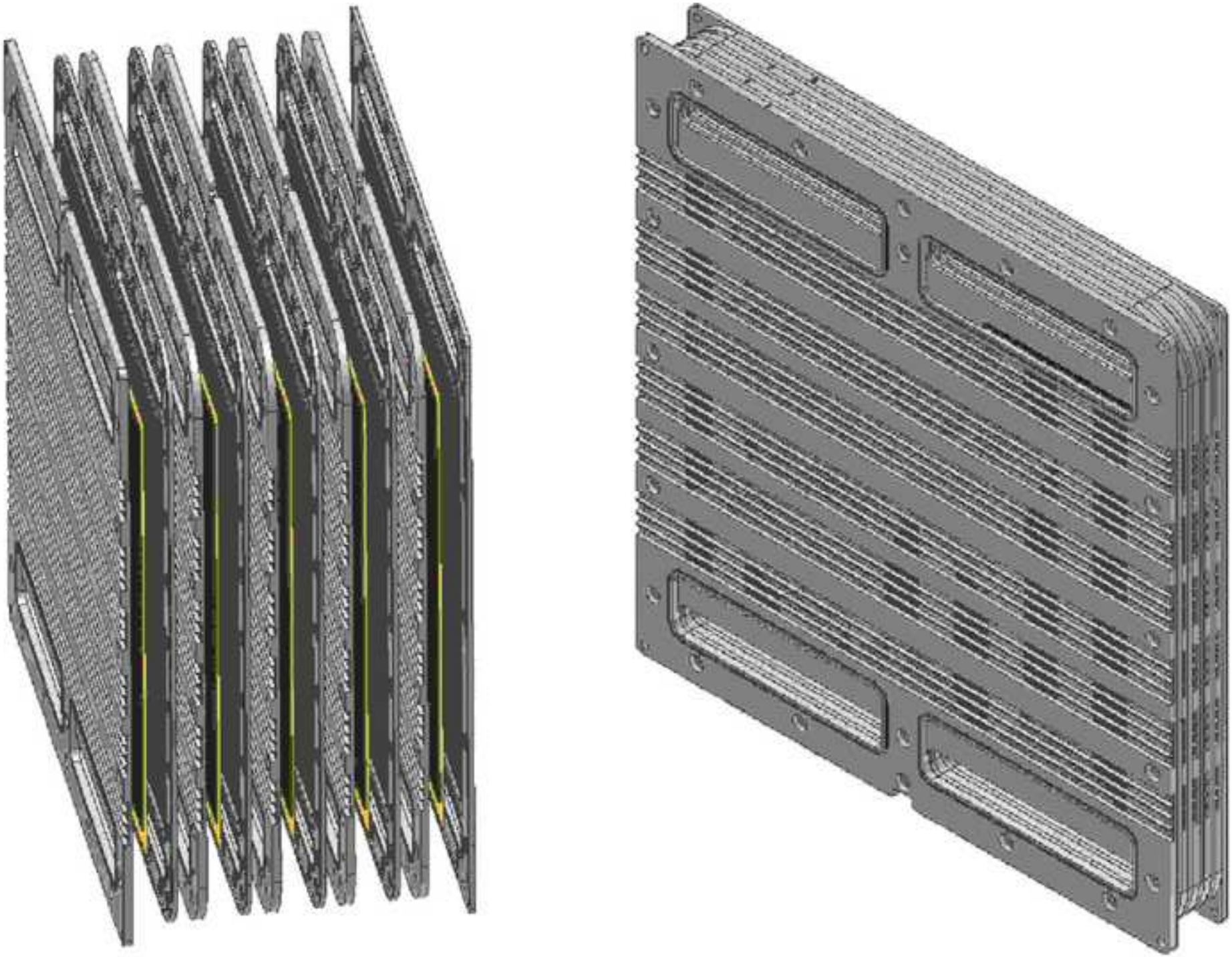

Fig-6

Click here to download high resolution image

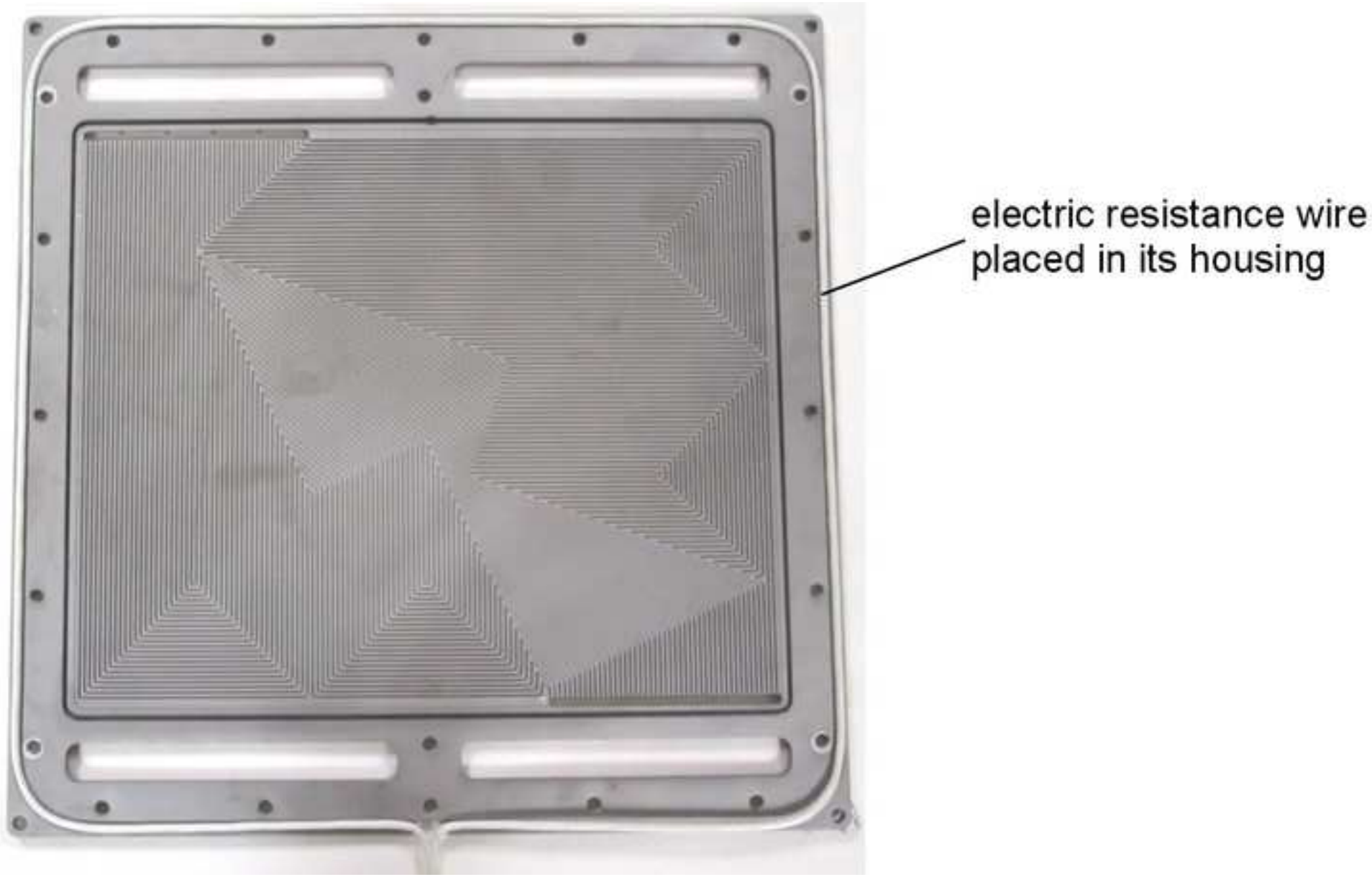

Fig-7

Click here to download high resolution image

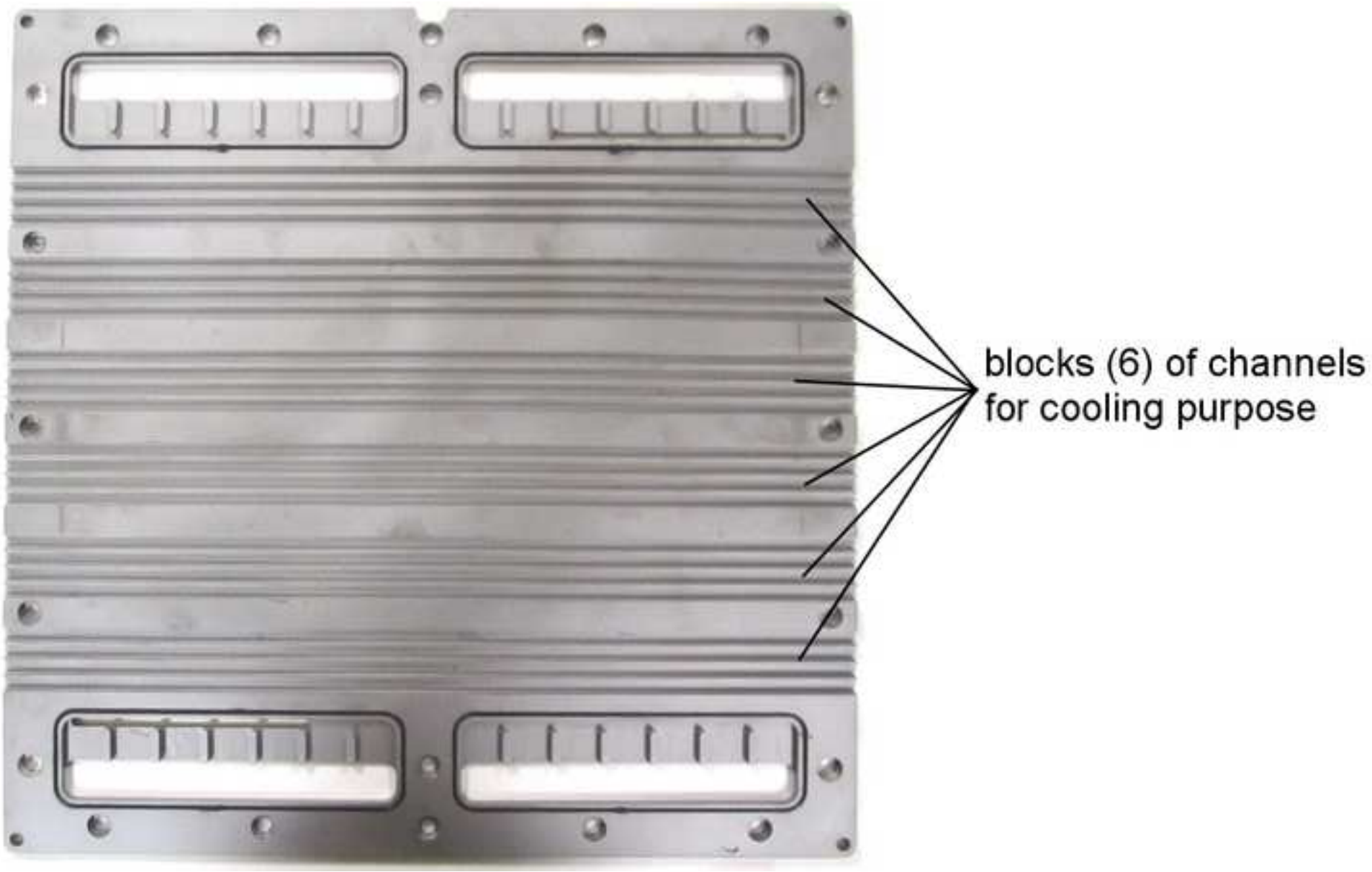

Fig-8

Click here to download high resolution image

Fig-9

Click here to download high resolution image

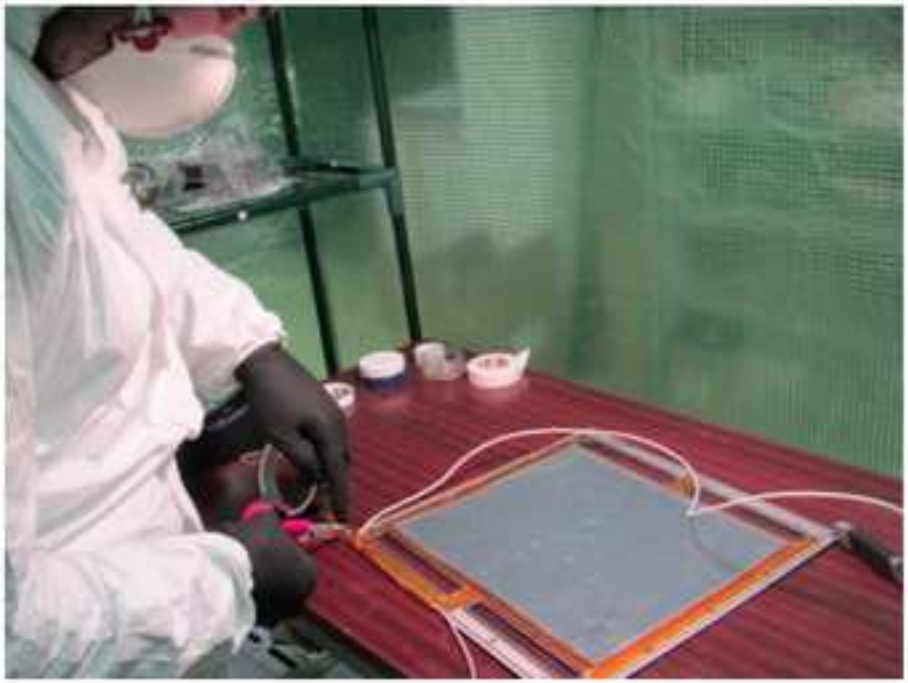

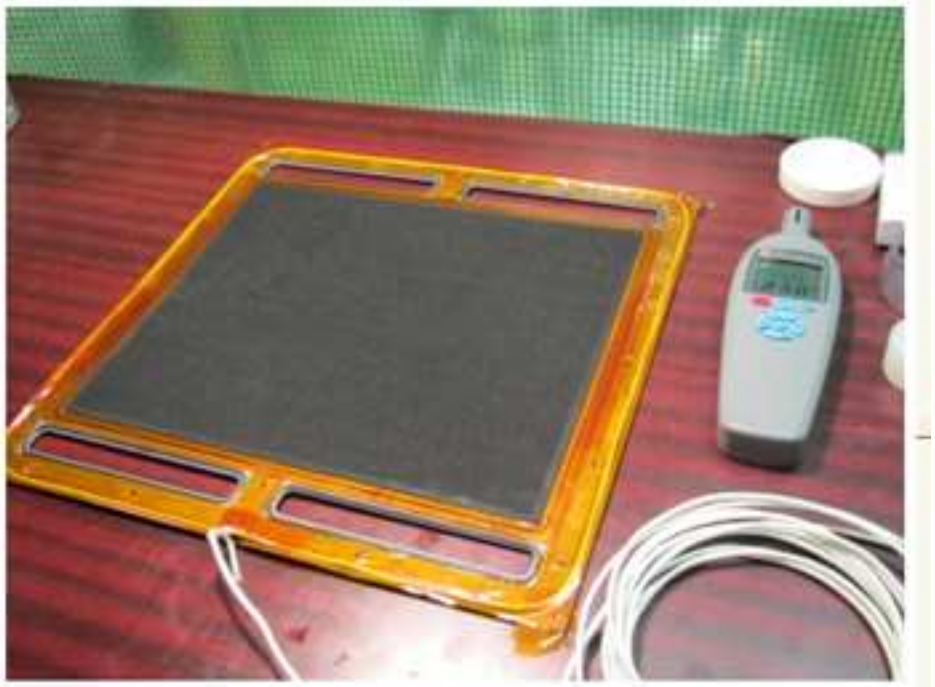

Fig-10

Click here to download high resolution image

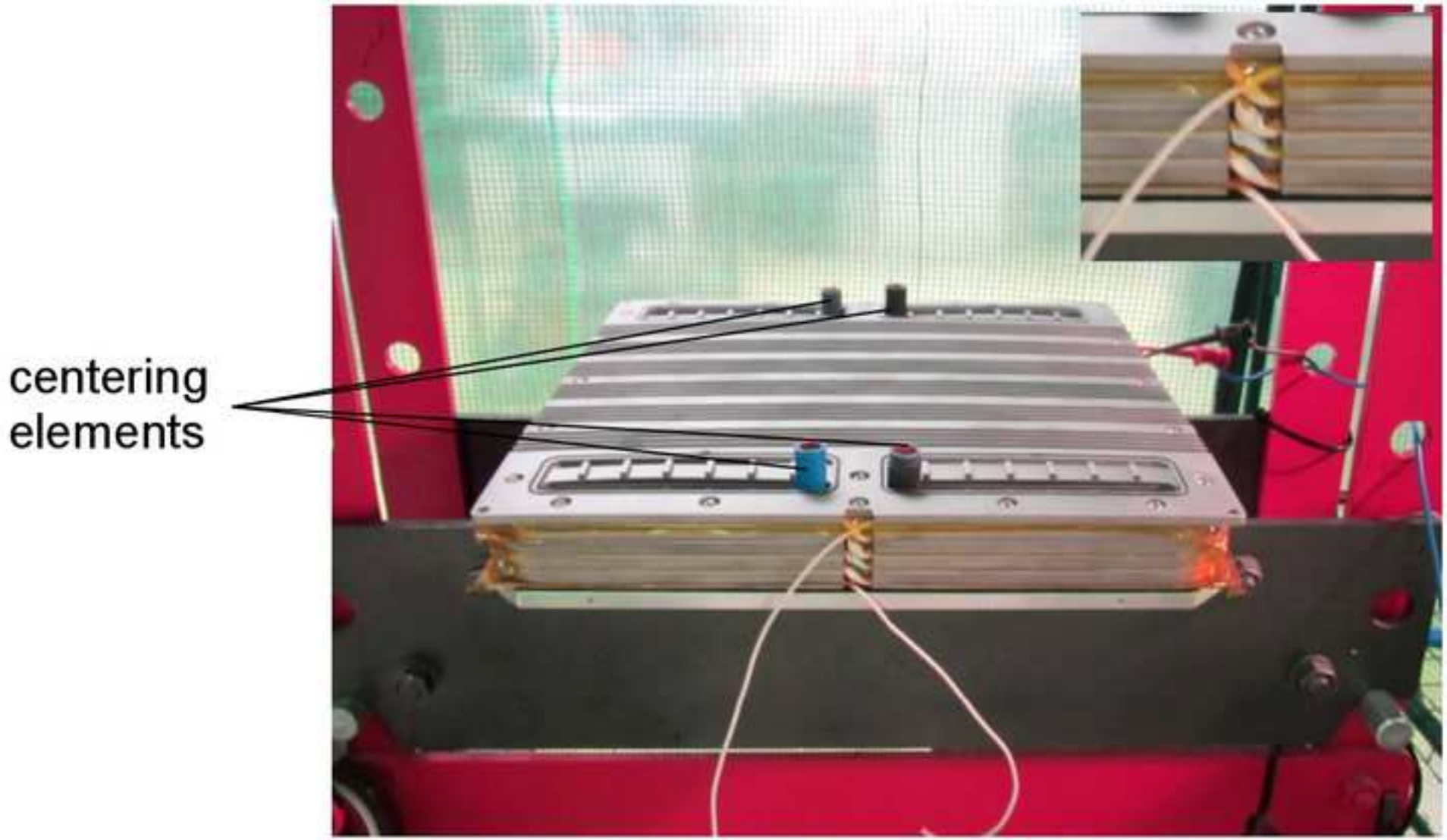

Fig-11

Click here to download high resolution image

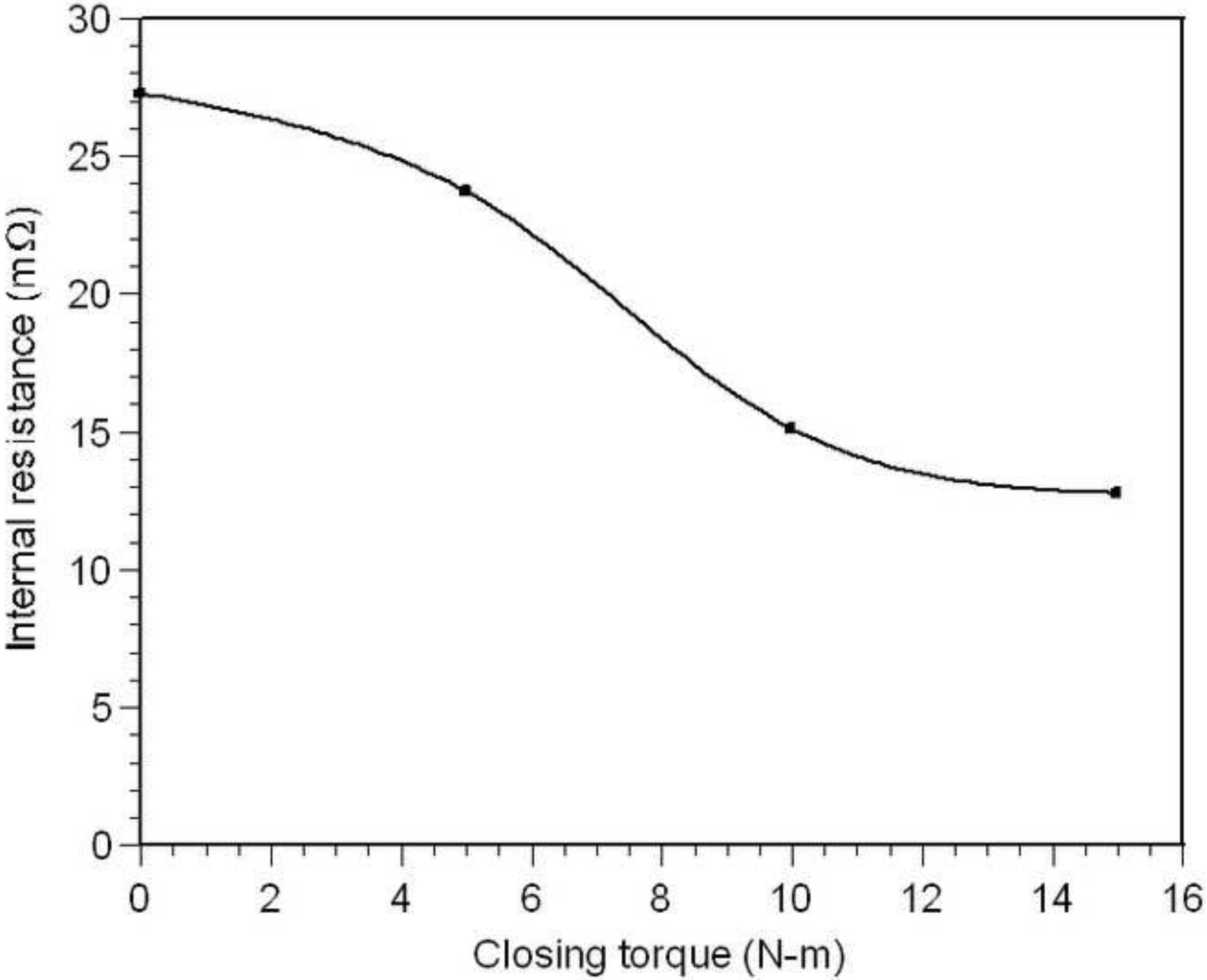

New Fig-12
Click here to download high resolution image

a)

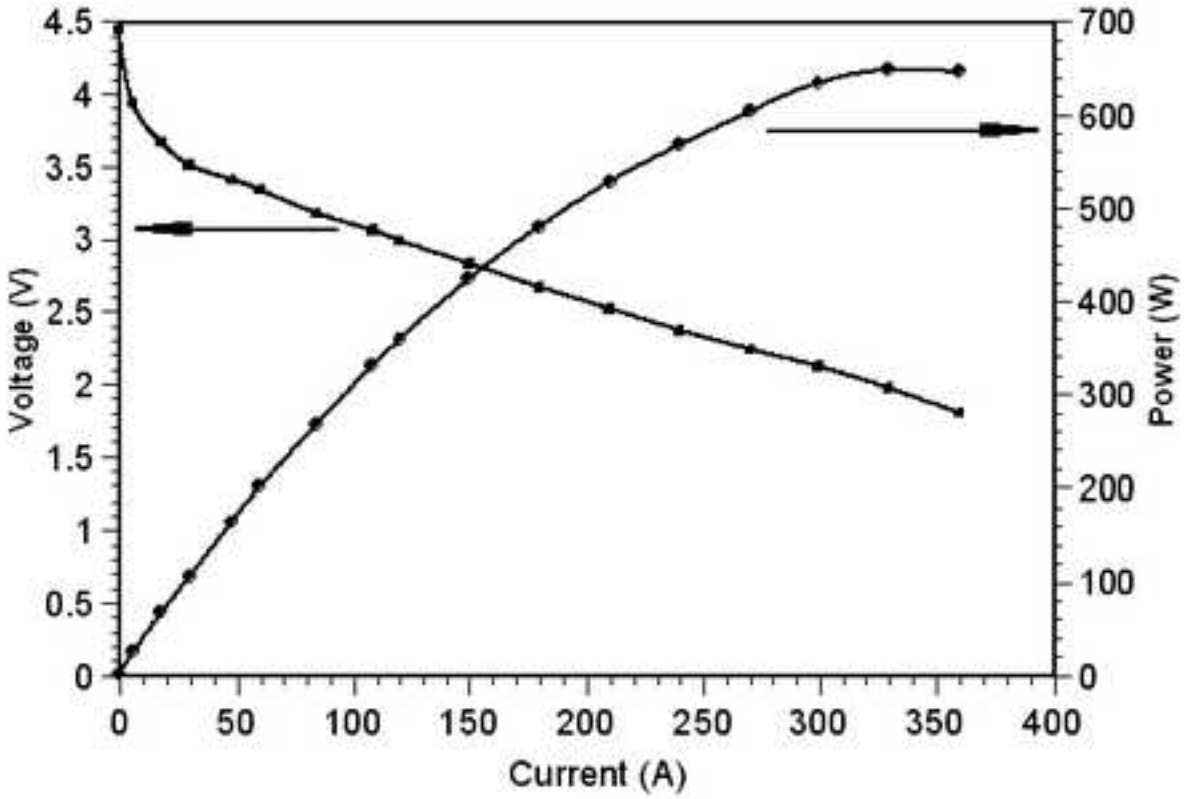

b)